Photoacoustic and Ultrasonic Tomography for Breast Imaging

Felix Lucka and the PAMMOTH team

Note: *This is an extended abstract of a talk I gave on May 4, 2023, at the Oberwolfach Workshop 2318 on "Tomographic Inverse Problems: Mathematical Challenges and Novel Applications". It is part of the Oberwolfach Workshop Report 2023, 21. The original slides of the talk contain much more material and references and can be found here, and an updated and extended version can be found here. I decided to upload this excerpt of the workshop report to arXiv because colleagues could not find it online. If you want to cite it, please check whether the corresponding full length publication is on arXiv or published in the meantime.*

New high-resolution, three-dimensional imaging techniques are being developed that probe the breast without delivering harmful radiation and without requiring painful compression. In particular, photoacoustic tomography (PAT) and ultrasound tomography (UST) promise to give access to high-quality images of tissue parameters with important value for the detection and diagnosis of breast cancer. However, the involved inverse problems are very challenging from an experimental, mathematical and computational perspective. In this talk, we want to give an overview of these challenges and illustrate them with data from an ongoing clinical feasibility study that uses the PAMMOTH scanner for combined PAT and UST.

Mathematically, the forward problem of PAT can be modeled in four steps: Firstly, the breast is illuminated by a short pulse of near-infrared laser light. The transport, scattering and absorption of photons in the breast tissue can be modeled by the radiative transfer equation (RTE):

$$(v \cdot \nabla + \mu_a(x) + \mu_s(x))\, \Phi(x,v) = q(x,v) + \mu_s(x) \int \Theta(v,v')\Phi(x,v')\, dv' \tag{1}$$

Here, $\Phi(x,v)$ denotes the photon transport density in location x and direction v, μ_a and μ_s denote absorption and scattering coefficients, q models the laser source and Θ is the scattering kernel. The photoacoustic effect describes how the rapid absorption of the optical energy leads to a thermoelastic expansion of the tissue, which induces a pressure increase:

$$p_0(x) = \Gamma(x)\mu_a(x) \int \Phi(x,v')\, dv' \quad , \tag{2}$$

where Γ describes the efficiency of this conversion of optical into acoustic energy. The initial pressure p_0 travels through the tissue as ultrasonic waves

$$\big(c(x)^{-2}\partial_t^2 - \Delta\big)\, p(x,t) = 0, \qquad p(x,0) = p_0(x), \qquad \partial_t p(x,0) = 0 \tag{3}$$

which can be measured once they reach the detection surface of the scanner:

$$f = Mp \tag{4}$$

PAT inversion consists of two coupled inverse problems: First, ones tries to recover p_0 from f, which corresponds to solving an acoustic initial value problem (3) with

boundary data (4). More details on this linear inverse problem can be found in [1]. We formulate its solution as a variational regularization problem

$$\min_{p_0 \in \mathcal{C}} \|MAp_0 - f\|_W^2 + \mathcal{R}(p_0) \quad , \tag{5}$$

where the linear operator A maps p_0 to the solution of (3), and use first-order optimization schemes with early stopping (*accelerated proximal gradient descent*, see [2] for more details). We illustrate how using accurate models of the ultrasound transducers improve the reconstructed images, validate the results using experimental phantoms and show *in-vivo* results of volunteers and patients, cf. Fig 1. In a second step, we try to recover μ_a from p_0, which corresponds to an optical parameter identification problem (1) with internal data (2). More details on this non-linear inverse problem can be found in [3].

In UST, we emit ultrasonic waves from $i = 1, \dots, N_s$ sources supported on the measurement surface and capture the transmitted and scattered waves as

$$f_i = M_i p_i, \qquad \left(c(x)^{-2}\partial_t^2 - \Delta\right) p_i(x,t) = s_i(x,t), \qquad p(x,0) = \partial_t p(x,0) = 0 \tag{6}$$

Recovering the *speed-of-sound* c from $\{f_i\}_{i=1}^{N_s}$ is an acoustic parameter identification problem with boundary data. There are different approaches to solve this non-linear inverse problem, typically accounting for different aspects of the complex wave physics underlying the data generation. For instance, *travel time tomography* is based on a geometrical optics approximation and relies on travel time differences of the transmitted waves as the main source of information. It leads to a robust and computationally efficient inversion scheme, see [4] for more details. However, the approximation limits the spatial resolution obtainable. *Time-domain full waveform inversion* (*TD-FWI*) relies on numerical wave solvers and formulates the solution to (6) as a variational regularization problem

$$\min_{c \in \mathcal{C}} \sum_{i}^{N_s} \|M_i \underbrace{\left(c(x)^{-2}\partial_t^2 - \Delta\right)^{-1} s_i(x,t)}_{p_i(c)} - f_i\|_2^2 + \mathcal{J}(c) \quad . \tag{7}$$

To solve this large-scale, non-convex optimization problem via first-order optimization schemes, the adjoint state method can be used to compute

$$\nabla_c \|M_i p_i(c) - f_i\|_2^2 = 2 \int_0^T c(x)^{-3} \partial_t^2 p_i(x,t) q_i^*(x,t)\, dt \quad , \tag{8}$$

where $q_i^*(x,t)$ solves $\left(c(x)^{-2}\partial_t^2 - \Delta\right) q^*(x,t) = s^*(x,t)$ and $s^*(x,t)$ is time-reversed data discrepancy $M_i p_i - f_i$. For high resolution 3D UST (~ 0.5mm isotropic resolution), using TD-FWI holds three key challenges: Firstly, the computation of the gradient for a single source i has a restrictively large memory footprint. Secondly, the number of sources N_s used in the PAMMOTH patient protocol is 18.000. Lastly, the structure of (7) may result in slow progression of the solver and convergence to a local minimum. We describe a comprehensive computational strategy to overcome these challenges in [5], discuss its translation to experimental data

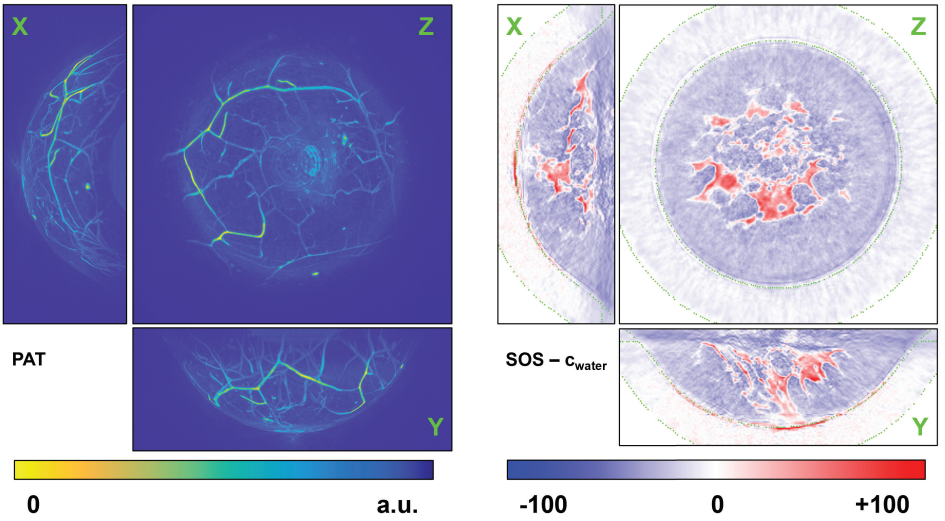

FIGURE 1. Examples of preliminary *in-vivo* results. Left: 3D reconstruction of p_0 with a spatial resolution of 0.4mm, visualized as maximum intensity projections. Right: 3D reconstruction of $c - c_{water}$ using TD-FWI with a spatial resolution of 0.6mm, visualized as slice views.

and illustrate preliminary results for experimental phantoms and breast cancer patients, *cf.* Fig 1.

REFERENCES

[1] P. Kuchment, L. Kunyansky, *Mathematics of Photoacoustic and Thermoacoustic Tomography*, Handbook of Mathematical Methods in Imaging (O. Scherzer) **32** (2011), 817–865.

[2] S.R. Arridge, M.M. Betcke, B.T. Cox, F. Lucka, B.E. Treeby, *On the adjoint operator in photoacoustic tomography*, Inverse Problems **32(11)** (2016), 115012.

[3] B. Cox, J.G. Laufer, S.R. Arridge, P. Beard *Quantitative spectroscopic photoacoustic imaging: a review*, Journal of Biomedical Optics **17(6)** (2012), 061202-1–061202-22.

[4] A. Javaherian, F. Lucka, B.T. Cox, *Refraction-corrected ray-based inversion for three-dimensional ultrasound tomography of the breast*, Inverse Problems **36(12)** (2020), 125010.

[5] F. Lucka, M. Pérez-Liva, B.E. Treeby, B.T. Cox, *High resolution 3D ultrasonic breast imaging by time-domain full waveform inversion*, Inverse Problems **38(2)** (2021), 025008.